Received 5 April 2009
Revised 3 September 2009
Accepted 27 October 2009

Properties of steady-state solutions for a simulated solid rocket motor

Michael Shusser
Department of Mechanical Engineering,
Technion – Israeli Institute of Technology, Haifa, Israel

Abstract

Purpose – This paper's aim is to propose a quasi-steady numerical model of a solid rocket motor that includes the coupling of motor chamber gas dynamics with the composite solid propellant combustion.

Design/methodology/approach – The paper considers a model problem of steady-state burning of a pure monopropellant coupled with a quasi-steady gas dynamic model of the combustion chamber. In order to simulate the time evolution as the propellant burns back with time, the flow-field in the chamber, the burning rate and the linear response function parameters are calculated for three port diameters of a simple cylindrical geometry.

Findings – It is shown that the pressure-coupled linear response function remains approximately constant along the propellant surface but can change very strongly as the chamber pressure rises due to increase in the burn surface.

Research limitations/implications – Only simplified motor geometry is considered but more realistic geometries can also be analyzed using a similar approach.

Originality/value – This study is the first step in building a comprehensive fully coupled model for numerical simulation of the internal flow-fields of solid rocket motors. In addition, it demonstrates how to use the steady-state results to calculate linearized pressure-coupled response of the propellant.

Keywords Motion, Dynamics, Rocket engines, Gas flow
Paper type Research paper

Nomenclature

A	dimensionless parameter characteristic of surface decomposition
A_{ox}	kinetics prefactor for AP surface decomposition
a	area
B	dimensionless parameter characteristic of the coupling of the gas phase and the surface
E_{ox}	activation energy of AP surface decomposition
E_s	activation energy of exothermic condensed phase reaction
F	thrust
H_{ox}	dimensionless heat release from the AP flame
n	burn rate pressure exponent
p	pressure
p_{atm}	atmospheric pressure
R	universal gas constant
R_p	pressure-coupled response function
r	burning rate
T_s	AP surface temperature
T_0	initial propellant bulk temperature
V_x	axial velocity
β_p	fraction of exothermic reactions that occur in the gas phase

Many helpful discussions with Norman Cohen are gratefully acknowledged.

International Journal of Numerical Methods for Heat & Fluid Flow
Vol. 20 No. 8, 2010
pp. 910-923

0961-5539
DOI 10.1108/09615531011081432

λ	complex frequency	ρ	gas density
ξ_{ox}	dimensionless AP flame height	ρ_{ox}	AP density

The overbar denotes steady-state values and the primed quantities are their perturbations.

1. Introduction

Understanding of combustion of solid propellants is a basis for analyzing, predicting and suppressing of combustion instabilities in solid rocket motors. The main cause of these instabilities is the response of the combustion process to pressure oscillations in the combustion chamber. Hence, the most important physical quantity characterizing unsteady combustion is the response of mass burning rate to pressure oscillations.

Stability of solid rocket motors and combustion chamber flow-fields have been studied by many authors. Among the recent analytical and numerical works one can mention Balachandar *et al.* (2001), García-Schäfer and Liñán (2001), Apte and Yang (2002), Flandro and Majdalani (2003), Kurdyumov (2006), Flandro *et al.* (2007), Shimada *et al.* (2008) and Massa (2009). More references can be found in these papers and in the review of Culick and Yang (1992).

However, most studies of combustion dynamics of solid propellants in rocket motors concentrated on propellant burning or on gas dynamics of the flow-field in the combustion chamber. Sophisticated models of both phenomena have been developed (Rasmussen and Frederick, 2002; Apte and Yang, 2002). By themselves, however, the models considered so far allow one to calculate combustion response to imposed pressure perturbations or to calculate the flow in the combustion chamber for imposed propellant burning rate. For example, Shusser *et al.* (2002a, b, 2008) suggested sophisticated combustion models for ammonium perchlorate (AP) and AP composite propellants but calculated their combustion response only for imposed pressure perturbations. No influence of burning rate perturbations on the pressure in the combustion chamber could be studied within the framework of their models.

To analyze the stability of solid propellant combustion in a rocket motor, it is necessary to include the coupling of motor chamber gas dynamics with the combustion process at the boundaries of the flow-field. The standard work in this area has been the Levine and Baum nonlinear instability code (Baum and Levine, 1983), which coupled one-dimensional gas dynamics with a simple and heuristic representation of the combustion. Although able to describe features of nonlinear instability observed in research motors, the Levine and Baum one-dimensional model is inadequate to represent most motor geometries of practical interest, and its combustion model does not contain mechanisms to isolate the key propellant variable of oxidizer particle size or the key flow variable of turbulent interaction. Thus, there is need to evolve to two-dimensional gas dynamics coupled with a composite propellant model.

The first step in building a comprehensive fully coupled model for numerical simulation of the internal flow-fields of solid rocket motors would be to consider steady-state burning of composite solid propellant coupled with a quasi-steady gas dynamic model of the combustion chamber. However, the importance of such calculation goes beyond that. In addition, one can use the steady-state results to calculate linearized pressure-coupled response of the propellant.

Small perturbation analysis of unsteady combustion of a homogeneous propellant (Culick, 1968) yields the following classical analytical solution for the pressure-coupled response function R_p:

$$R_p \equiv \frac{r'\overline{p}}{\overline{r}p'} = \frac{nAB}{\lambda + A/\lambda - 1 - A(1-B)} \tag{1}$$

Here p is the pressure, r is the burning rate, the overbar denotes steady-state values and the primed quantities are their perturbations, λ is a non-dimensional complex frequency of oscillations, while each of the basic parameters n, A, B characterizes the dependence of the steady-state burning rate on a certain physical quantity. Thus, the pressure exponent n characterizes the dependence on pressure, A (characteristic of the surface decomposition) is related to the dependence on the surface temperature, and B (characteristic of the heat feedback law) shows the dependence on the surface temperature gradient, i.e. heat flux.

Since the parameters A, B, n are determined by the steady-state solution one can calculate the linear response functions from the steady-state calculations. Performing a series of quasi-state calculations we can obtain the variation of the linear response function over the propellant surface and its evolution with time.

Analyzing the linear response of AP composite propellants Shusser *et al.* (2008) demonstrated that a composite propellant requires a more complicated description where both AP and binder have their own set of basic parameters n, A, B describing the relations between corresponding surface temperatures, heat fluxes and burning rates. In addition, both oxidizer and binder have their own response functions.

One would like to begin the analysis from a simpler case of a homogeneous propellant. To use it for future composite propellant calculations, we first consider a model problem of steady-state burning of a simulated energetic monopropellant coupled with a quasi-steady gas dynamic model of the combustion chamber. To simulate the time evolution as the propellant burns back with time, we perform the calculation for three port diameters, using a simple cylinder grain geometry in order to show a large pressure change with time. We will use the steady-state solution to calculate the pressure-coupled response of the propellant and we will see from the results that the linear response function can change very strongly.

Since a model problem with a simulated monopropellant is considered in this work, one might ask about the applicability of the results to real practical propellants.

First of all, monopropellant ingredient results, as for an oxidizer powder, can have implications for propellants because the monopropellant flame can control the propellant behavior at high pressures (Cohen and Strand, 1982).

Second, we show the practical result of the need to avoid combustion control by high-pressure-dependent kinetics flames because that would force the need to limit ourselves to grain geometries that have very small burn area changes.

2. Model

We consider a solid rocket motor with the main dimensions shown in Figure 1. The nozzle entrance diameter was 0.12 m and the nozzle throat diameter was 0.089 m. For simplicity and to show a large pressure variation, a cylindrical propellant grain with the aft end at the nozzle entrance was assumed.

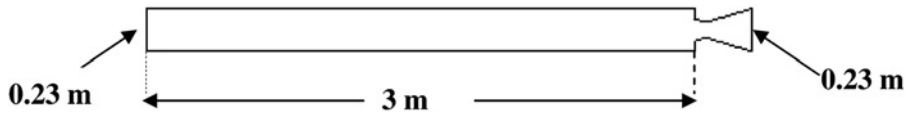

Figure 1.
Dimensions of the considered solid rocket motor

The Cohen and Strand AP monopropellant model (Cohen and Strand, 1982, 1985a, b) was used to calculate the steady-state propellant combustion. The obtained values of the steady-state burning rate were used to calculate the response function (1). The expressions for the response function parameters A, B, n were obtained in Shusser *et al.* (2002a) by linearizing the Cohen and Strand model and are written out in the Appendix for convenience.

The gas dynamic calculation was made with a commercial CFD code FLUENT (Fluent Inc., Lebanon, NH, USA) for axisymmetric compressible turbulent flow of an ideal gas. The k-ω model was used for turbulence modeling. The gas properties were taken from Culick and Yang (1992) and are summarized in Table I. The previously described computer code for the Cohen and Strand model (Shusser *et al.*, 2002b) was coupled with FLUENT by defining it as compiled UDF and provided the boundary condition for the mass flux at the propellant surface. The temperature of the gas entering the chamber was assumed constant and equal to 3,000 K. The last assumption is justified since monopropellant flame temperatures depend on pressure only slightly (Cohen and Strand, 1982; 1985a, b).

The discretization was coupled-implicit and of the second order. There were about 5,000 cells in the grid with some changes for different geometries. Mesh refinement tests showed that this value was satisfactory. For example, doubling the number of grid cells changed the values of the n, A, B parameters only slightly. To obtain good initial approximation, a preliminary calculation with a constant propellant mass flux was done first. This way, very good convergence was usually achieved with the residuals of about 10^{-12}.

Due to strong dependence of monopropellant burning rates on pressure even slight changes in the port diameter have considerable influence on the burning rate. Therefore, the calculations were done for three close values of the propellant port diameter: the initial diameter of 0.16 m, the intermediate diameter of 0.174 m and the final diameter of 0.19 m. These three cases will be referred to as "Start", "Intermediate" and "End" in the paper. The results of the calculations are given below.

3. Results

The pressure distribution along the combustion chamber and nozzle axis is shown in Figure 2. Due to the increase in burn surface and the high-pressure exponent ($n \sim 0.9$), the pressure is about five times higher for the final port diameter than for the initial port diameter. On the other hand, the pressure changes only slightly along the combustion chamber axis, most of the changes being in the nozzle. Although the pressure varies considerably for the three cases in Figure 2 the shape of the curve looks similar in all the cases. Indeed, if we normalize the pressure by its upstream value the curves become very close, as can be seen in Figure 3.

Axial velocity and temperature distributions along the combustion chamber and nozzle axis are shown in Figures 4 and 5. Here also the change between the three cases is rather limited. This is due to the fact that the propellant temperature is the same in all the cases and therefore the temperature and axial velocity distribution in the nozzle is mainly defined by geometry of the nozzle. One also sees from the figure that the gas

c_p (J/(kg·K))	k (W/(m·K))	μ (kg/(m·s))	M (kg/kmole)
2,020	0.2083	$8.25 \cdot 10^{-5}$	25

Table I.
Gas properties

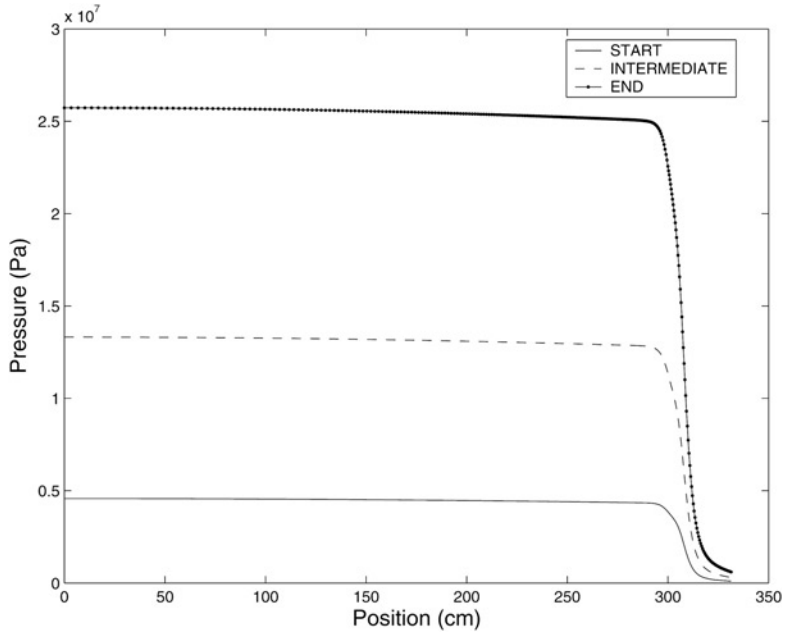

Figure 2.
Pressure distribution along the motor axis

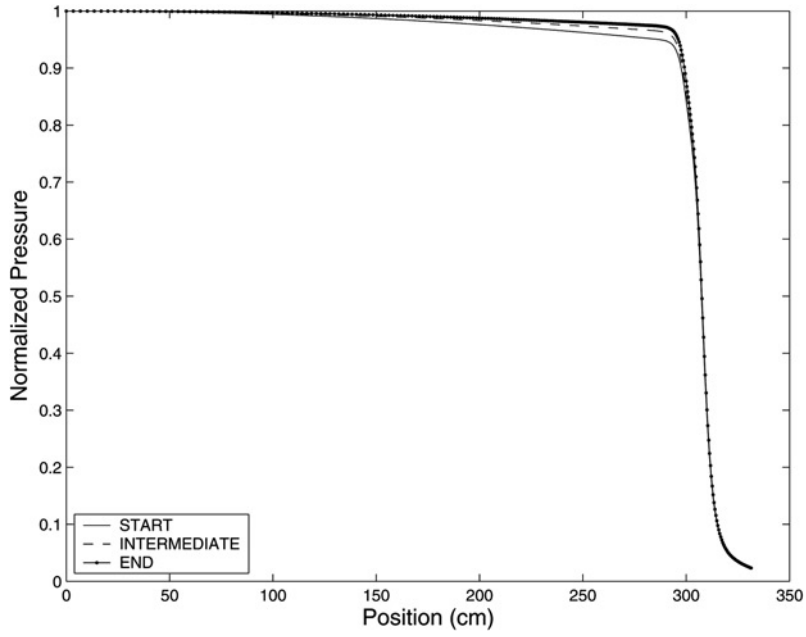

Figure 3.
Normalized pressure distribution along the motor axis

velocity in the chamber remains small. Therefore, the gas temperature in the combustion chamber is practically constant and begins to drop only in the nozzle.

Radial distributions of pressure, normalized pressure, Mach number and temperature at the nozzle exit are shown in Figures 6-9. The pressure

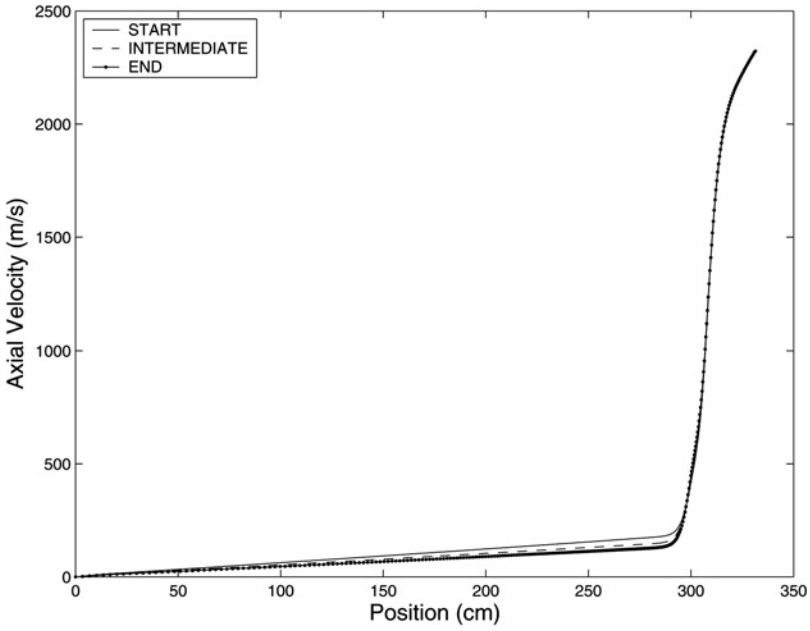

Figure 4.
Axial velocity distribution along the motor axis

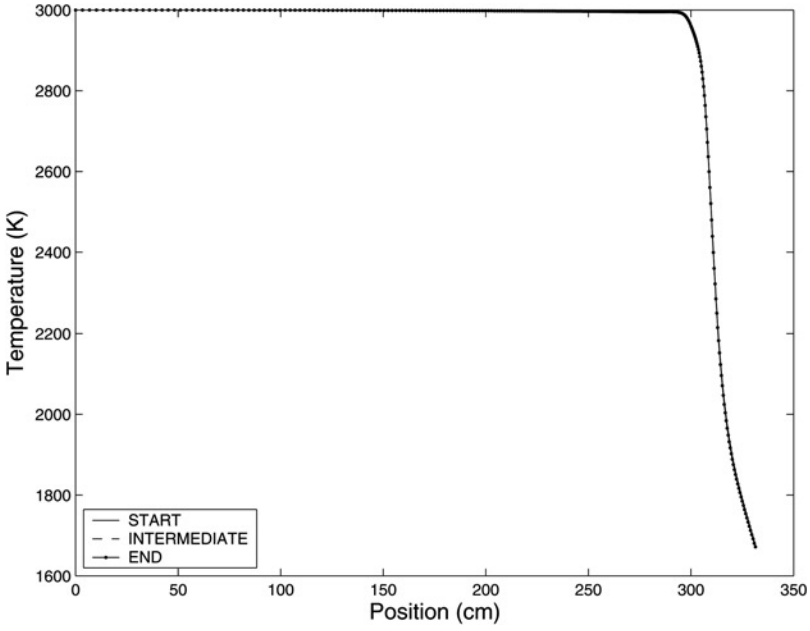

Figure 5.
Temperature distribution along the motor axis

was normalized by its value at the axis. We see that the distributions are similar to the previous plots. The pressure strongly increases with the port diameter while the normalized pressure, the Mach number and the temperature remain very close.

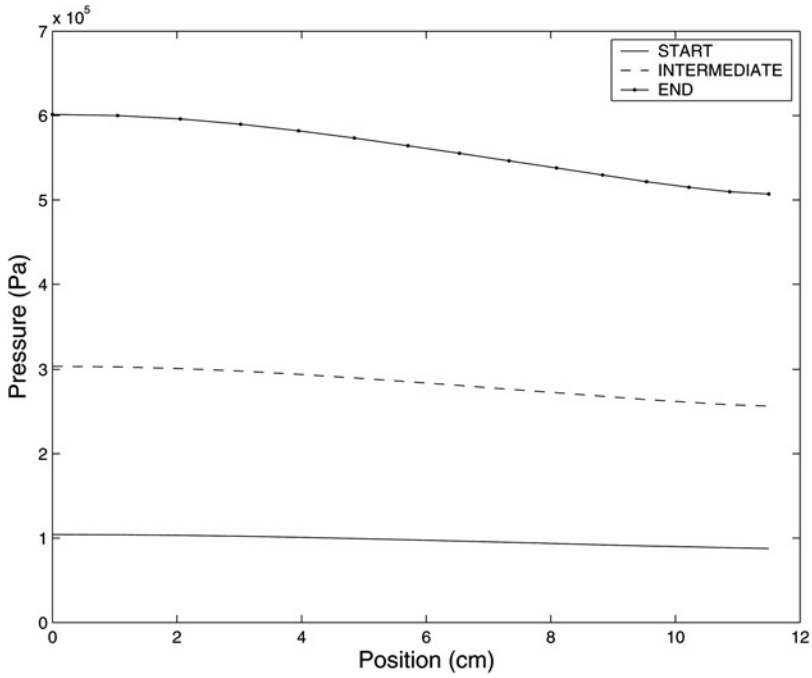

Figure 6.
Radial pressure distribution at the nozzle exit

The thrust was calculated for the three cases using the following expression obtained from the conservation of momentum:

$$F = \int_{outlet} (p - p_{atm} + \rho V_x^2) da \tag{2}$$

The results are shown in Table II. They demonstrate that the thrust increases very strongly as the propellant burns back.

Distributions of the pressure and the burning rate along the propellant surface are shown in Figures 10 and 11. It is seen that in the problem considered the burning rate changes very little over the propellant surface but increases from about 0.55 cm/s initially to about 2.7 cm/s in the end.

Knowing the pressure and the burning rate at the propellant surface we can calculate the linear response function parameters A, B, n using the relations given in the Appendix. The distribution of the parameters along the propellant surface is shown in Figures 12-14 and the average values are given in Table III.

One sees from the results that for each case all the parameters vary very little over the propellant surface and can be assumed constant for all practical purposes. In addition, the A and n parameters change only slightly between the initial and the final port diameters despite the large increase in pressure. On the other hand, the average value of the B parameter over the propellant surface decreases from 0.91 at the start to 0.65 at the end. The reason for the large change is the decrease in the flame height with the increasing pressure causing stronger coupling between the flame and the surface (Shusser *et al.*, 2002a).

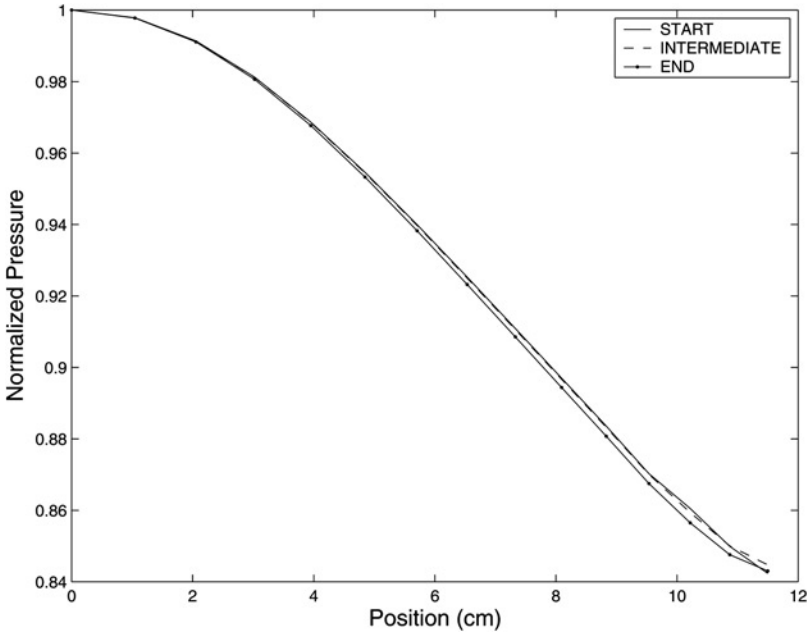

Figure 7.
Radial normalized pressure distribution at the nozzle exit

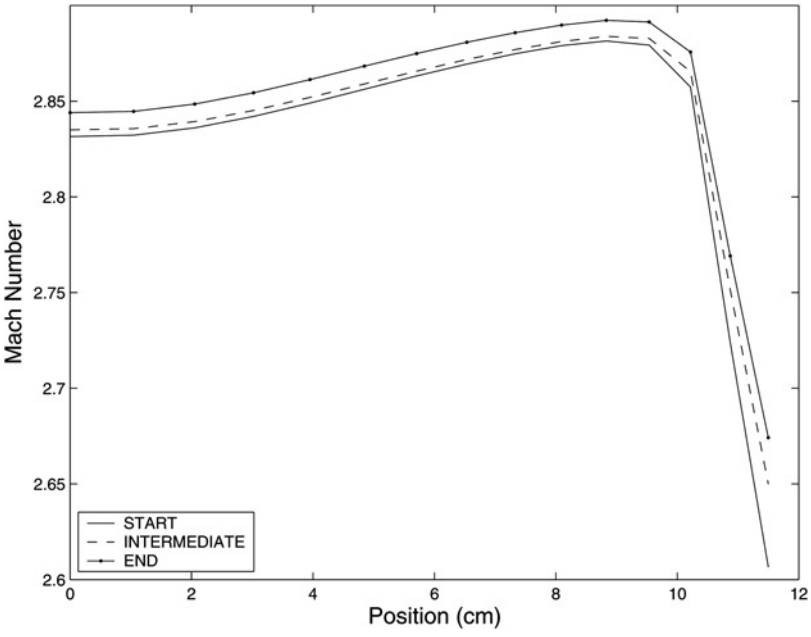

Figure 8.
Radial Mach number distribution at the nozzle exit

The observed large change in the B parameter has a strong influence on the pressure-coupled response function (Culick, 1968; Shusser *et al.*, 2002a). The pressure-coupled linear response function is plotted for the three cases in Figure 15. The main result is that the response function changes drastically as we go from the initial to the final port diameter.

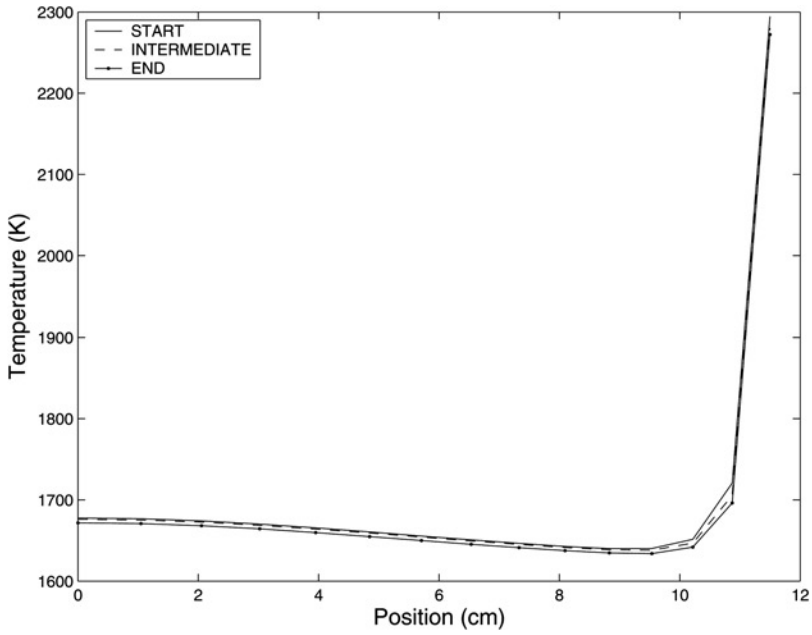

Figure 9.
Radial temperature distribution at the nozzle exit

Case	Thrust (*N*)
Start	36,152
Intermediate	113,892
End	230,747

Table II.
Thrust evolution

As the value of the B parameter decreases, the response function curve becomes more peaked and its maximum value grows from about 3 to approximately 24. Thus, the "End" case is much more prone to instability.

The very strong response obtained for the final port diameter suggests that we are close to the boundary of intrinsic instability. According to the classical theory (Culick, 1968) the intrinsic instability arises when the denominator of Equation (1) vanishes. This results in the following criterion:

$$\frac{A(1-B)^2}{1+B} > 1 \tag{3}$$

The average value of left-hand side of Equation (3) is shown in the last column of Table III. It is seen that the "End" case is indeed close to intrinsic instability.

4. Conclusions

This work considered a model problem of steady-state burning of a simulated monopropellant coupled with a quasi-steady gas dynamic model of the combustion chamber. The calculations were done for three port diameters to simulate the time

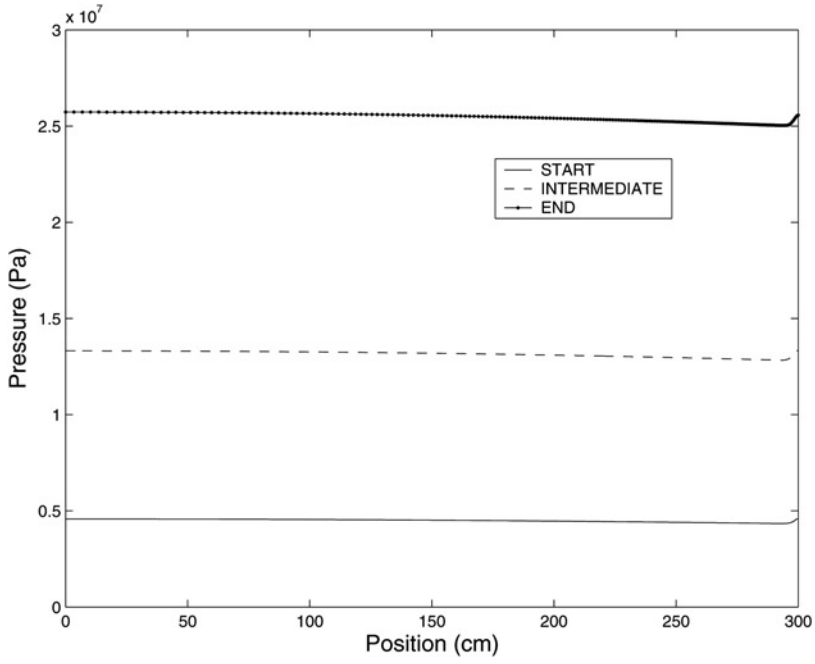

Figure 10.
Pressure distribution along the propellant surface

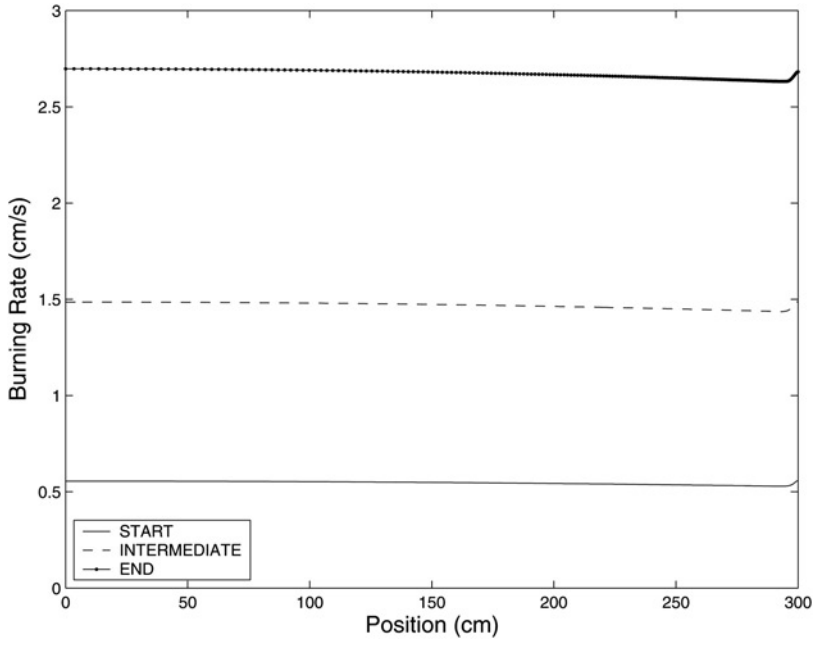

Figure 11.
Burning rate distribution along the propellant surface

evolution as the propellant burns back. The details of the flow-field in the chamber and in the nozzle were obtained. In addition, the calculation yielded the distribution of the burning rates and the linear response function parameters A, B and n over the propellant surface.

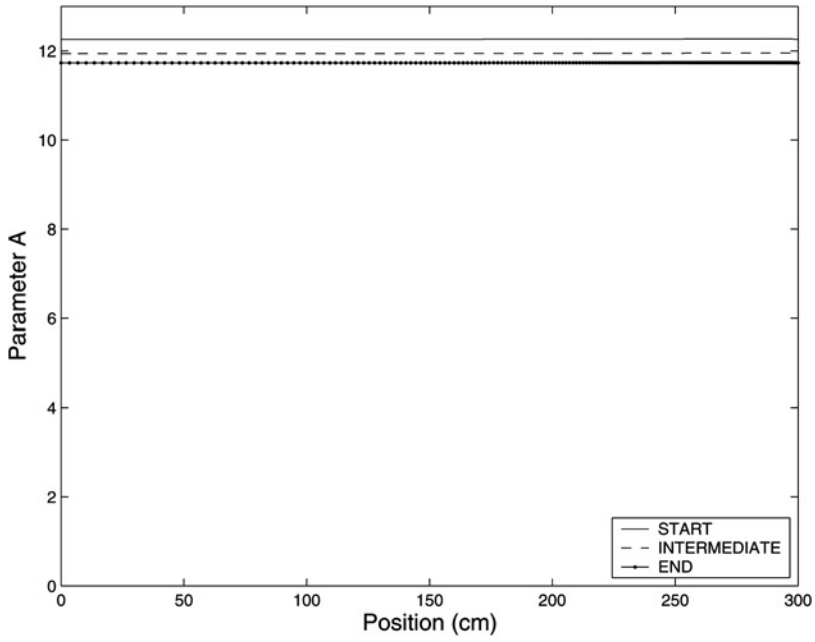

Figure 12.
Parameter A distribution along the propellant surface

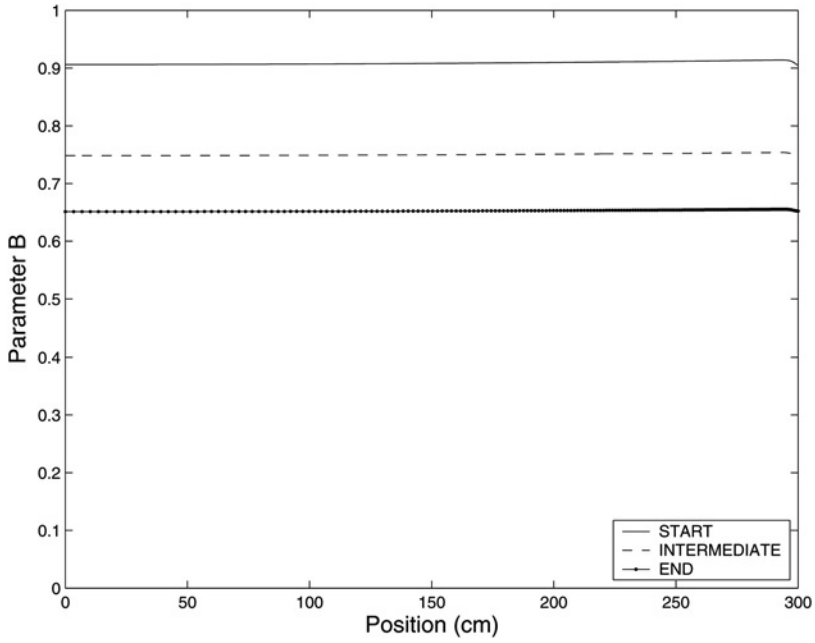

Figure 13.
Parameter B distribution along the propellant surface

The main result of the paper is the finding that the linear response function remains approximately constant along the propellant surface but can change very strongly as pressure increases. The reason for this is the decrease in the value of the

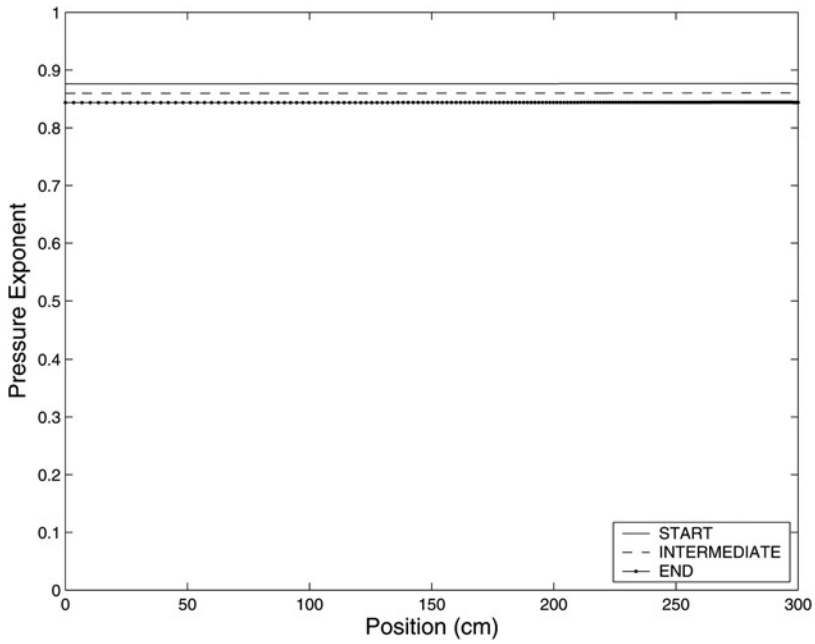

Figure 14.
Parameter n distribution along the propellant surface

Case	A	B	n	$A(1-B)^2/(1+B)$
Start	12.3	0.91	0.88	0.052
Intermediate	11.9	0.75	0.86	0.425
End	11.7	0.65	0.84	0.869

Table III.
Average values of response function parameters

B parameter as the chamber pressure increases due to the larger burn surface. The controlling factor is the reduced flame height with increasing pressure. On the other hand, the A and n parameters were found to be rather insensitive to even a large pressure change.

It should be noted that no strong effect of the axisymmetric flow was found in this work, as the flow parameters did not change much along the motor axis. One of the reasons for this is the simplified motor geometry. More importantly, the propellant combustion model used in this work did not include the flow effects, such as erosive burning. It is known that proper modeling of erosive burning may often require 2D or 3D flow models (see e.g. Willcox *et al.*, 2007).

Future work will be extended to AP composite propellants in which a verified composite propellant combustion model will be used for coupling to the gas dynamics of the motor, and will progress from steady-state to non-steady combustion/flow calculations.

It is anticipated that oxidizer/binder diffusion flame control in the composite propellants will promote stabilization.

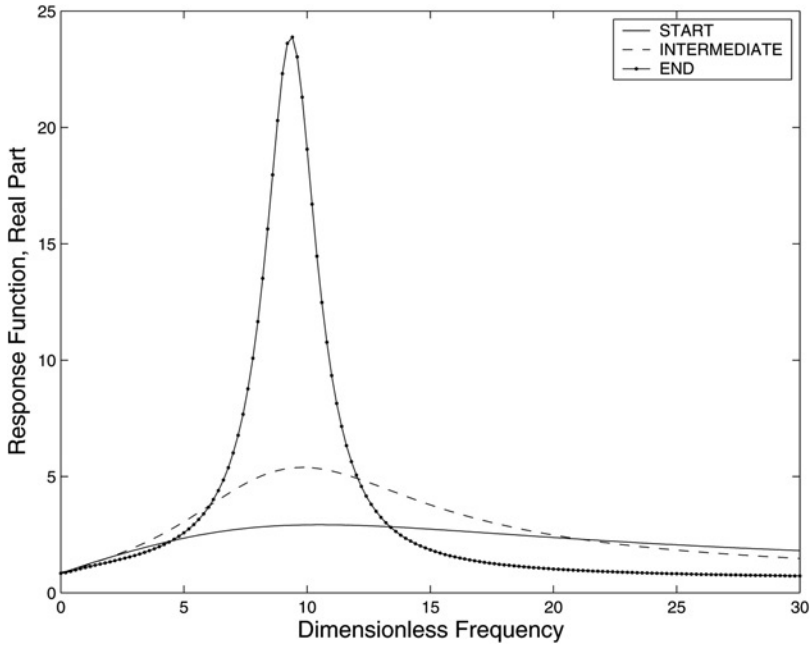

Figure 15.
Response function for different port diameters

References

Apte, S. and Yang, V. (2002), "Unsteady flow evolution and combustion dynamics of homogeneous solid propellant in a rocket motor", *Combustion and Flame*, Vol. 131 Nos 1/2, pp. 110-31.

Balachandar, S., Buckmaster, J.D. and Short, M. (2001), "The generation of axial vorticity in solid-propellant rocket-motor flows", *Journal of Fluid Mechanics*, Vol. 429, pp. 283-305.

Baum, J.D. and Levine, J.N. (1983), *Modeling of Nonlinear Combustion Instability in Solid Propellant Rocket Motors*, Report AFRPL-TR-83-058, US Air Force Research Laboratory, Edwards AFB, Edwards, CA.

Cohen, N.S. and Strand, L.D. (1982), "An improved model for the combustion of AP composite propellants", *AIAA Journal*, Vol. 20 No. 12, pp. 1739-46.

Cohen, N.S. and Strand, L.D. (1985a), "Combustion response to compositional fluctuations", *AIAA Journal*, Vol. 23 No. 5, pp. 760-7.

Cohen, N.S. and Strand, L.D. (1985b), "Effect of AP particle size on combustion response to crossflow", *AIAA Journal*, Vol. 23 No. 5, pp. 776-80.

Culick, F.E.C. (1968), "A Review of calculations for unsteady burning of a solid propellant", *AIAA Journal*, Vol. 6 No. 12, pp. 2241-55.

Culick, F.E.C. and Yang, V. (1992), "Stability predictions in rocket motors", in De Luca, L., Price, E.W. and Summerfield, M. (Eds), *Nonsteady Burning and Combustion Stability of Solid Propellants*, AIAA, Washington, DC, Ch. 18, pp. 719-79.

Flandro, G.A. and Majdalani, J. (2003), "Aeroacoustic instability in rockets", *AIAA Journal*, Vol. 41 No. 3, pp. 485-97.

Flandro, G.A., Fischbach, S.R. and Majdalani, J. (2007), "Nonlinear rocket motor stability prediction: limit amplitude, triggering, and mean pressure shift", *Physics of Fluids*, Vol. 19, Article No. 094101.

García-Schäfer, J.E. and Liñán, A. (2001), "Longitudinal acoustic instabilities in slender solid propellant rockets: linear analysis", *Journal of Fluid Mechanics*, Vol. 437, pp. 229-54.

Kurdyumov, V.N. (2006), "Steady flows in the slender, noncircular, combustion chambers of solid propellant rockets", *AIAA Journal*, Vol. 44 No. 12, pp. 2979-86.

Massa, L. (2009), "Spatial linear analysis of the flow in a solid rocket motor with burning walls", *Combustion and Flame*, Vol. 156 No. 4, pp. 865-88.

Rasmussen, B. and Frederick, R.A. (2002), "Non-linear heterogeneous model of composite solid propellant combustion", *Journal of Propulsion and Power*, Vol. 18 No. 5, pp. 1086-92.

Shimada, T., Hanzawa, M., Morita, T., Kato, T., Yoshikawa, T. and Wada, Y. (2008), "Stability analysis of solid rocket motor combustion by computational fluid dynamics", *AIAA Journal*, Vol. 46 No. 4, pp. 947-57.

Shusser, M., Culick, F.E.C. and Cohen, N.S. (2002a), "Combustion response of ammonium perchlorate", *AIAA Journal*, Vol. 40 No. 4, pp. 722-30.

Shusser, M., Culick, F.E.C. and Cohen, N.S. (2002b), "Combustion response of AP composite propellants", *Journal of Propulsion and Power*, Vol. 18 No. 5, pp. 1093-100.

Shusser, M., Culick, F.E.C. and Cohen, N.S. (2008), "Analytical solution for pressure-coupled combustion response functions of composite solid propellants", *Journal of Propulsion Power*, Vol. 24 No. 5, pp. 1058-67.

Willcox, M.A., Brewster, M.Q., Tang, K.C., Stewart, D.S. and Kuznetsov, I. (2007), "Solid rocket motor internal ballistics simulation using three-dimensional grain burnback", *Journal of Propulsion Power*, Vol. 23 No. 3, pp. 575-84.

Appendix

The following expressions for the response function parameters A, B, n can be obtained by linearizing the Cohen and Strand model (Shusser *et al.*, 2002a):

$$A = \frac{E_{ox}(T_s - T_0)}{RT_s^2} \tag{A.1}$$

$$B = H_{ox}\left[\left(1 - \frac{E_s}{E_{ox}}\right)\frac{(1-\beta_p)}{\beta_p}(1 - \exp(-\xi_{ox})) + 2\xi_{ox}\exp(-\xi_{ox})\right] + \frac{1}{A} \tag{A.2}$$

$$n = \frac{2H_{ox}\xi_{ox}\exp(-\xi_{ox})}{B} \tag{A.3}$$

The model assumes the Arrhenius relationship between the surface temperature and the burning rate:

$$r = \frac{A_{ox}}{\rho_{ox}}\exp\left(-\frac{E_{ox}}{RT_s}\right) \tag{A.4}$$

About the author

Michael Shusser is a Senior Lecturer, Department of Mechanical Engineering, Technion – Israeli Institute of Technology, Israel. Michael Shusser can be contacted at: shusser@technion.ac.il